Copyright ©2018 by the International Astronautical Federation (IAF). All rights reserved.

IAC-18-F1.2.3

In-flight calibration of nanosatellites inertia tensor: the algorithm and requirements for on-board sensors

Belokonov I.V.[a], Lomaka I.A[b]*

[a] *Space research Department, Samara University, 34 Moskovskoye shosse, Samara, Russian Federation 443086,* ibelokonov@mail.ru
[b] *Space research Department, Samara University, 34 Moskovskoye shosse, Samara, Russian Federation 443086,* igorlomaka63@gmail.com
* Corresponding Author

Abstract

The paper presents an approach to solving the problem of nanosatellite's the main central moments of inertia values estimation, which is considered to be a body of variable mass in the course of flight, using the differential evolution algorithm. As an example, a nanosatellite of the CubeSat3U format with a propulsion system whose working body is about 10% of its total mass is considered. When nanosatellite maneuvering, the mass of the nanosatellite is reduced, as a result the moments of inertia and the position of the center of mass change, which affects the operation of the algorithm for maintaining the required orientation in space and stabilizing the motion. The study showed that the accuracy of estimating the magnitudes of moments of inertia is less than 1%.
Keywords: nanosatellite, differential evolution, algorithm, propulsion unit

Nomenclature

T - measurement period;

Acronyms/Abbreviations

GYR – gyroscope;
MAG – magnetometer;
ADCS – attitude determination and control system;
ISS – International Space Station;
DE – differential evolution algorithm;
AWS – the coordinate system associated with the spacecraft;
AGS – the absolute geocentric coordinate system;
OCS – orbital coordinate system;
IGRF – International Geomagnetic Reference Field;
RMS – root mean square

1. Introduction

Today, in addition to solving educational problems [1], nanosatellites are gradually beginning to perform increasingly complex space missions, for example [2,3,4]. Constantly growing requirements for the functionality of nanosatellites led to the natural appearance of propulsion systems [5, 6], which significantly expand the capabilities of nanosatellites to implement complex space missions. However, according to statistics, the reliability of nanosatellites remains at a lower level compared to full-size space vehicles [7]. This is primarily due to the inexpensive commercial components used in their design.

Thus, the problem arises of maintaining the stable operation of nanosatellite systems in the event of failure of one or more components. For example, ADCS is critical for missions that require precise orientation of the nanosatellite axes. For correct operation of this system, it is necessary to meet the following conditions: firstly, knowledge of the dynamic characteristics of the nanosatellite, and secondly, the correct operation of measuring instruments, controls, and on-board algorithms for determining attitude and control.

This paper considers an approach that makes it possible to estimate the main central moments of inertia from the accumulated information from one type of measuring sensors (in this work it is a gyroscope, an angular velocity sensor and light sensors).

A similar approach was used in [8], in which the moments of inertia of spacecraft were determined in flight when control actions were applied to the spacecraft with the help of flywheels and orientation engines, as data were used with GYR and accelerometer. A method for estimating the inertia tensor of the ISS is given in [9], but in this work the test actions of the control bodies were also used. In [10, 11] approaches are given to the reconstruction of the angular motion of the spacecraft by processing the readings of magnetometers; in the above articles, in addition to the parameters of the angular motion, the moments of inertia of the spacecraft are also estimated, and Gauss Newton and Levenberg Marquardt methods are used to solve problems. Thus, this work differs from the known ones in that the object of the study is a nanosatellite of the Cubesat 3U format and it is not necessary to apply special test actions.

The DE algorithm is used for numerical solution of the problem. The use of DE as a numerical method is due to the following reasons: firstly, the absence of the need to search for the initial approximation for the required parameters. Secondly, there is no need to calculate the partial derivatives of the minimized function, which

Copyright ©2018 by the International Astronautical Federation (IAF). All rights reserved.

allows you to get rid of time-consuming mathematical transformations and makes it possible to use more complex mathematical models of angular motion and measurement models. Third, an increase in the accuracy of the solution is achieved due to the lack of the need for the numerical determination of partial derivatives, and a search for a global extremum is provided, in contrast to the first and second order methods, which often find local extrema. The disadvantage of using DE is the large number of calls to the minimized function.

In this article, the proposed approach is illustrated by the example of SamSat-M nanosatellite (Fig. 1), developed at Samara University and designed to test the developed propulsion system [12].

Fig. 1. SamSat-M nanosatellite

Nanosatellite has a traditional set of sensors inertial information, as well as sensors of a different physical nature – MAG's and light sensors.

2. Problem formulation

Let there be a set of measurements from MAG β, the GYR τ and light sensors γ. The measurements are obtained during the time T - the measurement period.

It is required to obtain estimates of the main central moments of inertia of the nanosatellite (I_x, I_y, I_z). This problem reduces to the problem of non-linear multidimensional optimization, namely, to find the minimum of the objective function (1) (in case of using measurements from one type of sensor):

$$J(b) = \sum_{\alpha=xyz} \sum_{i=1}^{N} (\zeta_{\alpha i}(b) - \eta_{\alpha i})^2 \quad (1)$$

where $\zeta_{\alpha i}$ is the measurement model, b is the vector of the estimated parameters, $\eta_{\alpha i}$ is measurement, In this case, the vector of estimated parameters has the form:

$$b = [I_x, I_y, I_z] \quad (2)$$

In the process of preflight preparation, the moments of inertia of the nanosatellite can be determined with an accuracy of about 5%. As inputs to the operation of the numerical algorithm, accumulated measurements from sensors are used, as well as the range of permissible moments of inertia. Also, based on the energy balance of the satellite, it is possible to output one impulse per turn.

The following assumptions follow from these conditions:

• The moments of inertia on the satellite are known with an accuracy of 5%

• Model of the angular motion of the satellite takes into account the actions of the aerodynamic and gravitational moment

• Only the main central moments of inertia are determined

• The satellite is not a dynamic symmetric body

2.1 Rotation motion model

To write the equations of motion of the spacecraft around the center of mass (point O) (Fig. 2), as well as the relations used in data processing, three right Cartesian coordinate systems are introduced.

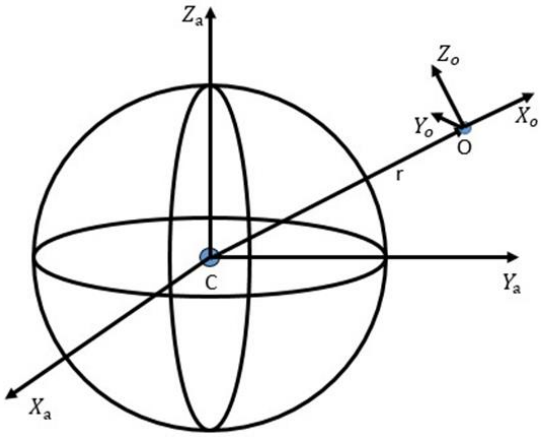

Fig. 2. Coordinate systems

The coordinate system (AWS) associated with the spacecraft is formed by the main central axes of inertia and has the designation $OX_cY_cZ_c$. The absolute geocentric coordinate system (AGS) has the designation $CX_aY_aZ_a$ a with the origin at the center of mass of the Earth (point C). The axis X_a is directed to the point of the vernal equinox. The axis Z_a is directed to the north pole of the world. The Y_a axis completes the system to the right. Orbital coordinate system (OCS) has the designation $OX_oY_oZ_o$. The beginning of the system is in the center of mass of the spacecraft. The X_o axis is directed along the RA radius vector. The axis Z_a is perpendicular to the plane of the orbit. The Z_a axis completes the system to the right.

OCS is obtained from AGS by three successive turns by an angle of longitude of the ascending node Ω around the axis Z_a, by the inclination angle i around the new axis X'_a and by the latitude argument u the new axis circle Z''_a. The position of the AWS relative to the OCS is given by three consecutive rotations through the precession angle ψ around the Y_o axis, the angle of attack α around the new axis Z'_o and by the angle of proper rotation φ around the new axis Y''_o.

The rotational motion of the space vehicle is described by the dynamical (3) and kinematic Euler

Copyright ©2018 by the International Astronautical Federation (IAF). All rights reserved.

equations (4). The right-hand sides of the dynamic Euler equations take into account the gravitational and aerodynamic moments. The equations of motion have the form:

$$\begin{gathered}\dot{\omega}_x = \mu\left(\omega_y\omega_z - \nu\, a_{21}a_{31}\right) + p\, E\left(r_y V_{cz} - r_z V_{cy}\right) S\,|V_c| \\ \dot{\omega}_y = \frac{1-\lambda}{1+\lambda\mu}\left(\omega_x\omega_z - \nu\, a_{31}a_{11}\right) + \frac{\lambda}{1+\lambda\mu} p\, E\left(r_z V_{cx} - r_x V_{cz}\right) S\,|V_c| \\ \dot{\omega}_z = -(1-\lambda+\lambda\mu)\left(\omega_x\omega_y - \nu\, a_{21}a_{11}\right) + \lambda\, p\, E\left(r_x V_{cy} - r_y V_{cx}\right) S\,|V_c|\end{gathered} \quad (3)$$

where $\lambda = \frac{I_x}{I_z}$ и $\mu = \frac{I_y - I_z}{I_x}$ – dimensionless inertia coefficients (the expressions for the dimensionless inertia coefficients are taken from [11];

$\nu = \frac{3\cdot\mu_e}{r^3}$ – gravitation torque coefficient;

$p = 0{,}5\,\rho\, C_x$ – drag coefficient;

S – the area of the projection of the nanosatellite surface onto a plane perpendicular to the velocity vector;

ρ - the density of the atmosphere at an altitude of nanosatellite orbit;

$\vec{V_c} = \left(V_{cx}\, V_{cy}\, V_{cz}\right)$ – orbital velocity vector;

$\vec{r} = \left(r_x\, r_y\, r_z\right)$ – vector directed from the center of mass to the center of pressure.

$$\begin{gathered}\frac{dq_0}{dt} = 0.5\cdot\left(-(\omega_x-\omega_{rx})\cdot q_1 - (\omega_y-\omega_{ry})\cdot q_2 - (\omega_z-\omega_{rz})\cdot q_3\right) \\ \frac{dq_1}{dt} = 0.5\cdot\left((\omega_x-\omega_{rx})\cdot q_0 + (\omega_z-\omega_{rz})\cdot q_2 - (\omega_y-\omega_{ry})\cdot q_3\right) \\ \frac{dq_2}{dt} = 0.5\cdot\left((\omega_y-\omega_{ry})\cdot q_0 + (\omega_x-\omega_{rx})\cdot q_3 - (\omega_z-\omega_{rz})\cdot q_1\right) \\ \frac{dq_3}{dt} = 0.5\cdot\left((\omega_z-\omega_{rz})\cdot q_0 + (\omega_y-\omega_{ry})\cdot q_1 - (\omega_x-\omega_{rx})\cdot q_2\right)\end{gathered} \quad (4)$$

where $\vec{\omega}_r = A(q)\cdot\begin{bmatrix}0\\0\\\omega_{\text{orb}}\end{bmatrix}$, ω_{orb} – spacecraft orbital angular velocity.

Transition matrix $A(q)$ is shown as follows

$$\begin{bmatrix}1-2\cdot(q_2\cdot q_2+q_3\cdot q_3) & 2\cdot(q_1\cdot q_2+q_3\cdot q_0) & 2\cdot(q_1\cdot q_3-q_2\cdot q_0)\\ 2\cdot(q_1\cdot q_2-q_3\cdot q_0) & 1-2\cdot(q_1\cdot q_1+q_3\cdot q_3) & 2\cdot(q_2\cdot q_3+q_1\cdot q_0)\\ 2\cdot(q_1\cdot q_3+q_2\cdot q_0) & 2\cdot(q_2\cdot q_3-q_1\cdot q_0) & 1-2\cdot(q_1\cdot q_1+q_2\cdot q_2)\end{bmatrix}$$

The motion model in the form (3) and (4) is convenient in that the vector r в enters it explicitly. This vector makes it possible to estimate the displacement of the center of mass of the spacecraft during the consumption of the working medium, since a single-valued correspondence can be obtained between the values of l_t and r ⃗.

2.2 Measurements models

Model of measurements of MAG. The magnetometer measurement model is a vector of the Earth's magnetic field $\vec{B}_{IGRF}$ [] calculated by the IGRF model. This vector is measured in the AWS, hence the vector $\vec{B}_{\text{meas}} = A\cdot\vec{B}_{IGRF}$ measured. We also add to the measured vector the measurement noise w_B, determined according to the normal law with a given RMS σ. Thus, the mathematical model of measurements of the magnetometer is written as:

$$\vec{B}_{\text{meas}} = A\cdot\vec{B}_{IGRF} + w_B(\sigma) \quad (5)$$

Model of measurements of the angular velocity sensor. The angular velocity measurement model is a solution of the system (1) $\vec{\omega}$ with the measurement noise w_a, determined according to the normal law with a given RMS σ. Thus, the mathematical model of the GYR measurements is written as:

$$\vec{\omega}_{\text{meas}} = \vec{\omega} + w_a(\sigma) \quad (6)$$

Model of measurements of the light sensor. The light sensor is a flat surface, the orientation of which is specified by the normal vector $\vec{n}$ in the AWS. The signal generated by the sensor is assumed to be proportional to the cosine of the angle of incidence of the sun's rays ⟦

$$I_{\text{dir}} = I_{max}\cdot\cos\left(\vec{n}\cdot\vec{S}\right) \quad (7)$$

In addition to taking into account the generation of the signal from direct solar radiation, described by the model (4), the current generated by the solar radiation reflected from the Earth is also taken into account in this work:

$$I_{\text{ref}} = I_{max}\cdot A_{\text{av}}\cdot\varphi_2 \quad (8)$$

where A_{av} is the average value of the Earth's albedo, φ_2 is the combined slope [13], I_{max} is the maximum value of the signal in this work $I_{max} = 1$. Also, the noise is added to the measurements w_L. Thus, the measurement model in this paper has the form

$$I = I_{\text{dir}} + I_{\text{ref}} + w_L \quad (9)$$

2.3 Algorithm of problem solution

The search for the minimum of the objective function (1) is carried out using DE [14], which consists in performing the following steps:

the assignment of the original array X consisting of N vectors b (N at each iteration is constant and is one of the parameters of the DE), each element of the vector b being randomly generated within the required limits;

generation of a new array X_{new} of vectors b: for each vector b_i from the array X randomly selected three different vectors $b_1, b_2, b_3, ,$ whose indices do not coincide with the index of the vector b_i, and the so-called modified vector (mutant vector) is calculated by the formula: $b_m = b_1 + F\cdot(b_2 - b_3)$, where F is a constant in the interval [0, 1], which is a parameter of the DE algorithm;

over the modified vector b_m, a "crossover" operation is performed, consisting in that some of its elements are replaced by the corresponding elements from the source vector b_i (each element is replaced with a probability P, which is also another parameter of the DE algorithm);

if the obtained vector is better than the vector b_i, that is, the value of the objective function decreases

Copyright ©2018 by the International Astronautical Federation (IAF). All rights reserved.

$J(b_t) < J(b_i)$, then in the new array X_{new} the vector b_i is replaced by the new vector b_t (called the test vector, trial vector), otherwise b_i;

paragraphs 1 to 4 repeat the specified number of iterations or until the required value of the minimized function is achieved.

3. An example of the application of the approach to a Cubesat 3U nanosatellite equipped with a propulsion system

Taking into account the motion model and the measurement model, it is necessary to change the vector of the estimated parameters (2), so that it contains not only the moments of inertia, but the parameters of the angular motion. The modified vector of the estimated parameters has the form

$$b = \left[\omega_x(t_0), \omega_y(t_0), \omega_z(t_0), \psi(t_0), \alpha(t_0), \varphi(t_0), \lambda, \mu, p\right]$$

where, $\omega_x(t_0), \omega_y(t_0), \omega_z(t_0)$ – angular velocity initial values, $\psi(t_0), \alpha(t_0), \varphi(t_0)$ – initial orientation angles, λ,μ - dimensionless inertia coefficients, p – aerodynamic coefficient.

With the known design of the spacecraft, it is possible to obtain the dependences of the coefficients λ and μ on the fuel level l_t, which makes it possible to shorten the vector of the estimated parameters, eliminating the values λ, μ from it, which positively affects the convergence of the optimization method. Thus, the vector of estimated parameters used in this problem has the form

$$b = \left[\omega_x(t_0), \omega_y(t_0), \omega_z(t_0), \psi(t_0), \alpha(t_0), \varphi(t_0), l_t, p\right]$$

Next, we obtain the dependences, $\lambda(l_t)$ and $\mu(l_t)$, using the example of a nanosatellite with a propulsion system, described in [12].

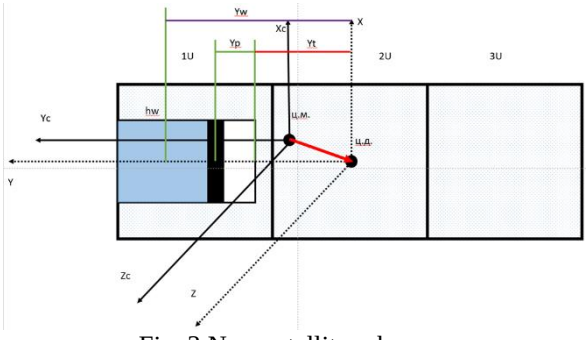

Fig. 3 Nanosatellite scheme

The calculation of the functions, , $\lambda(l_t)$ and $\mu(l_t)$, consists in determining the coordinates of the nanosatellite's center of mass, and then recalculating the moments of inertia by the Steiner theorem.

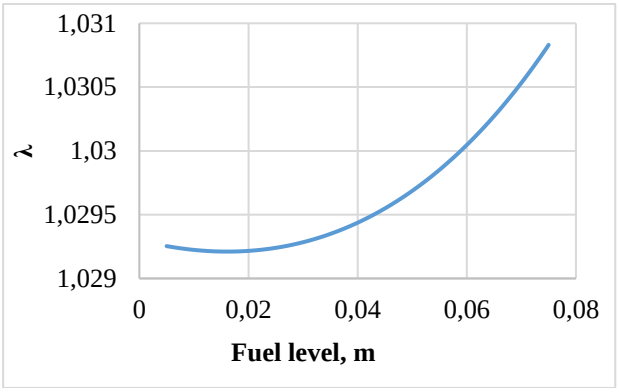

Fig. 4 Dependence $\lambda(l_t)$

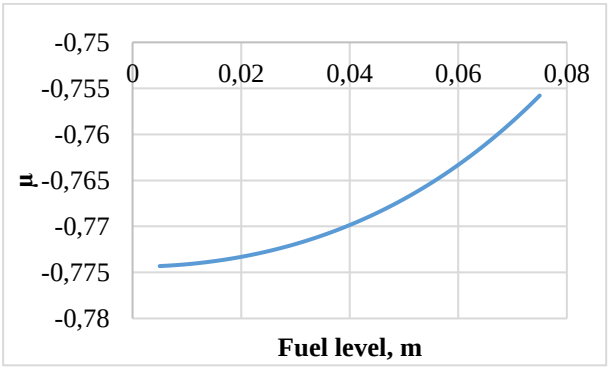

Fig. 5 Dependence $\mu(l_t)$

3.1 Simulation conditions

The algorithm was simulated under the following conditions:

- The angular velocity module does not exceed 1 deg / sec, the initial orientation angles lie in the range ± 20 degrees, which is ensured by the operation of the magnetic stabilization system.
- The simulation periods were 1 turn T, half the revolution 0.5T and a quarter turn 0.25T.
- The characteristics of the noise measurements of the sensors σ are given in the Table1 (Appendix A).
- The fuel level in the tank was 35mm which corresponds to half the capacity of the tank
- The moments of inertia of an empty nanosatellite are determined with an accuracy of 5%

Ground estimates are used as the range of allowable values for moments of inertia, so the estimates obtained as a result of the algorithm work are limited to ground-based estimates of moments of inertia

3.2 Simulation results

Let's estimate the maximum methodological error of the method in determining the level of fuel for various measuring sensors, which corresponds to a measuring period of 0.25T (Fig. 5), with increasing period, the

Copyright ©2018 by the International Astronautical Federation (IAF). All rights reserved.

method error decreases, as will be shown below, the error caused by measurement noise is also reduced. As can be seen from the plot, a method error with a probability of 0.95 does not exceed 0.03%. Results for different values of measurement noise are shown on Fig. 1, Fig. 2, Fig. 3 Appendix A.

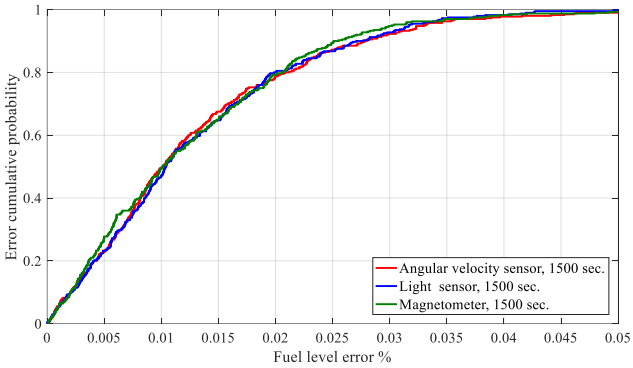

Fig. 5 Methodological error of the method

Moments of inertia of an empty nanosatellite can be determined on Earth with an accuracy of 5%. Thus, the moments of inertia of the nanosatellite with fuel will be the sum of the moments of inertia of the empty satellite and the moments of inertia of the fuel. We assume that the estimates of the moments of inertia are distributed according to the normal law. The distribution of the moments of inertia Ix Iz is shown in Fig. 6 and the moment Iy in Fig. 7.

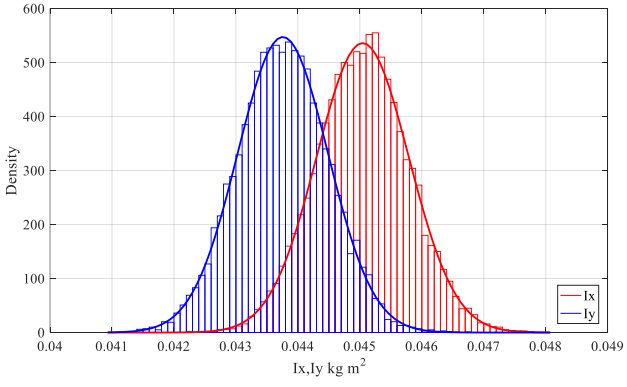

Fig. 6 Distribution of the moments of inertia Ix Iz

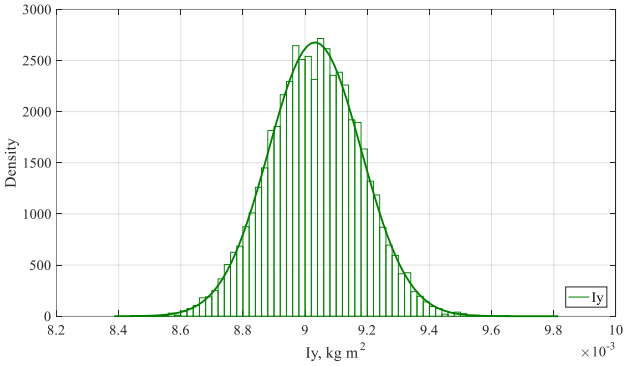

Fig. 7 Distribution of the moment of inertia Iy

Probabilistic characteristics of the estimated moments of inertia are presented in the table 1

Table 1 Probabilistic characteristics of the estimated moments of inertia

Inertia moment	Mean $\bar{I}$	Variance σ
Ix	0.04505	$5.5\ 10^{-7}$
Iy	0.00903	$2.2\ 10^{-8}$
Iz	0.04376	$5.4\ 10^{-7}$

As a result of the algorithm, fuel level estimates were obtained which, according to the functions $\lambda(l_t)$ and $\mu(l_t)$, were recalculated at moments of inertia. The resulting distribution of estimates is shown at Fig. 8 and Fig. 9. The distribution of the moments of inertia Ix Iz is shown in the Fig. 8. and moment Iy on the Fig. 9. These estimates are valid for angular velocity sensor and magnetometer since they have the same accuracy

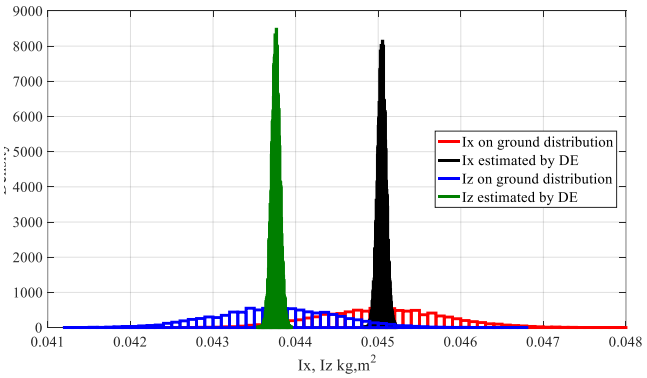

Fig. 8 Distribution of the moments of inertia Ix Iz

Copyright ©2018 by the International Astronautical Federation (IAF). All rights reserved.

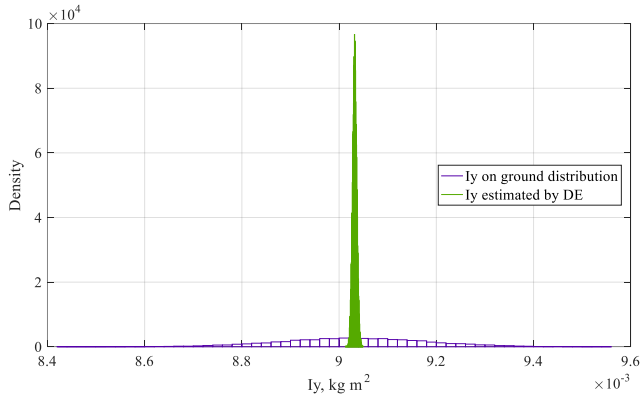

Fig. 9 Distribution of the moments of inertia Iy

The results for light sensors are shown below

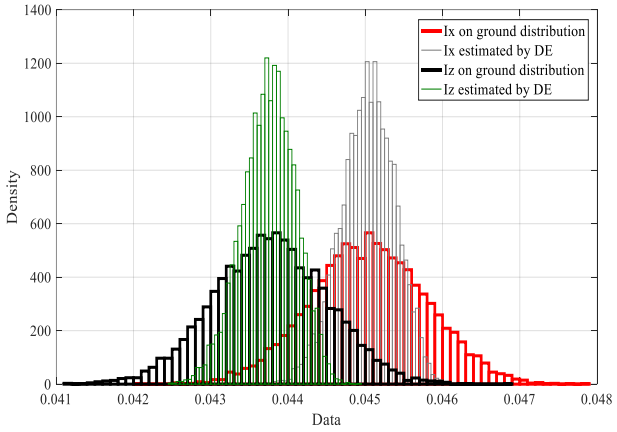

Fig. 10 Distribution of the moments of inertia Ix Iz

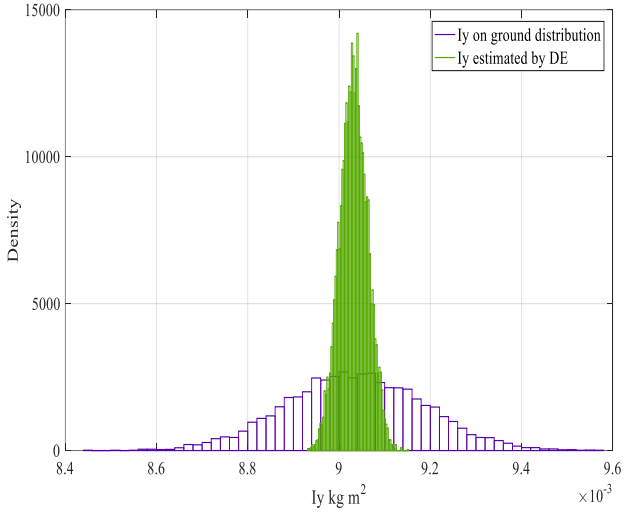

Fig. 11 Distribution of the moments of inertia Iy

The result values are shown in Table 2

Table 2 Probabilistic characteristics of the estimated moments of inertia

		Ix	Iy	Iz
Real values		0.045044	0.009032	0.043759
Testing stand	Mean $\bar{I}$ kg m^2	0.04505	0.00903	0.04376
	Variance σ kg m^2	5.5 10^{-7}	2.2 10^{-8}	5.4 10^{-7}
Magnetometer or angular velocity sensor	Mean $\bar{I}$ kg m^2	0.04504	0.00903	0.04376
	Variance σ kg m^2	1,9 10^{-9}	1,4 10^{-11}	1,8 10^{-9}
Light sensors	Mean $\bar{I}$ kg m^2	0.04503	0.00903	0.04376
	Variance σ kg m^2	1,2 10^{-7}	9 10^{-10}	1,17 10^{-7}

Thus, it can be seen that the use of light sensors does not significantly improve the accuracy of estimates of moments of inertia. This is due to the fact that the illumination sensors are periodically obscured due to the rotation of the nanosatellite. To improve the estimates it is necessary to carry out measurements over an interval of more than one turn. Using a magnetometer or gyroscope allows solving the problem in one turn.

4. Results

As a result of modeling, it is possible to form requirements for on-board nanosatellite measuring instruments. So it is necessary to use a scientific magnetometer with low measurement noise (not more than 75 nT), a problem can be solved with GYR (σ not more than 0.01 deg/s). When using light sensors, it is necessary to make measurements over a longer measurement interval.

5. Discussion

This approach can be useful in several cases: firstly, it can be applied in parallel with the standard control system algorithm, allowing in-flight to specify moments of inertia and use them in the control system, secondly, in case of abnormal situation on board (failure of the measurement system fuel level, incomplete disclosure or non-disclosure of solar cells), and thirdly, this method can be used to control the disclosure of solar cells or to monitor the operation of a propulsion system or any other event affecting change in the magnitude of the moments of inertia.

6. Conclusions

A requirements for on-board sensors were formed. It is shown that the problem can be solved on one orbital turn by using a gyroscope or a magnetometer.

Copyright ©2018 by the International Astronautical Federation (IAF). All rights reserved.

Acknowledgements

The research was carried out at the expense of a grant from the Russian Science Foundation (project No. 17-79-20215).

Appendix A (Simulation conditions)

Table 1. The characteristics of the noise measurements of the sensors σ

Sensor	Period	Noise σ	Plot index
Angular velocity	T	0 deg/s	A1.1
		0,001 deg/s	A1.2
		0,01 deg/s	A1.3
		0,1 deg/s	A1.4
	0.5T	0 deg/s	A2.1
		0,001 deg/s	A2.2
		0,01 deg/s	A2.3
		0,1 deg/s	A2.4
	0.25T	0 deg/s	A3.1
		0,001 deg/s	A3.2
		0,01 deg/s	A3.3
		0,1 deg/s	A3.4
Magnetometer	T	0 nT	M1.1
		75 nT	M1.2
		200 nT	M1.3
		500 nT	M1.4
	0,5 T	0 nT	M2.1
		75 nT	M2.2
		200 nT	M2.3
		500 nT	M2.4
	0.25 T	0 nT	M3.1
		75 nT	M3.2
		200 nT	M3.3
		500 nT	M3.4
Light	T	0%	L1.1
		2%	L1.2
		5%	L1.3
		10%	L1.4
	0.5T	0%	L2.1
		2%	L2.2
		5%	L2.3
		10%	L2.4
	0.25T	0%	L3.1
		2%	L3.2
		5%	L3.3
		10%	L3.4

Appendix B (Simulation results)

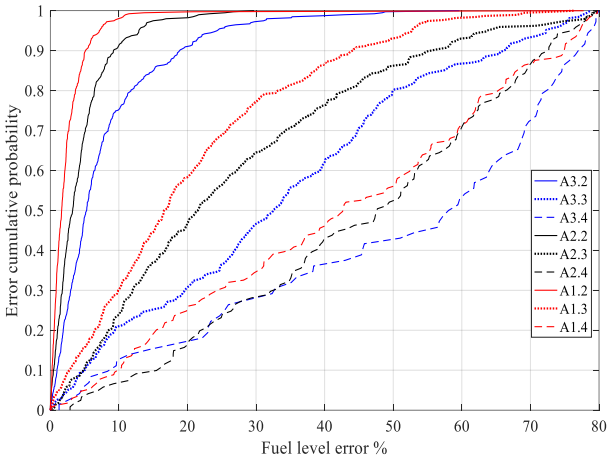

Fig. 1 Error cumulative probability for GYR

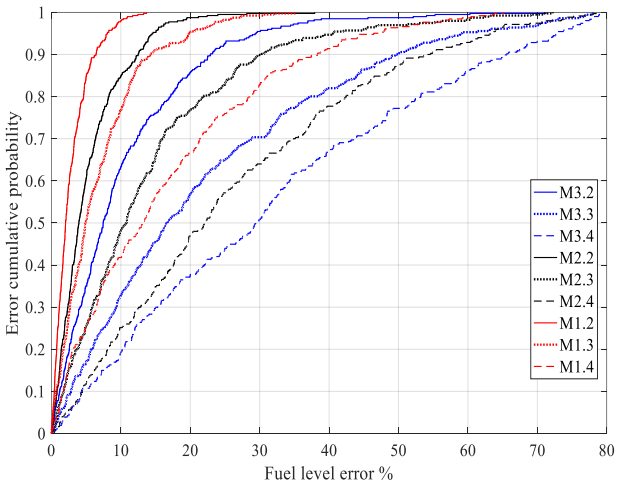

Fig. 2 Error cumulative probability for magnetometer

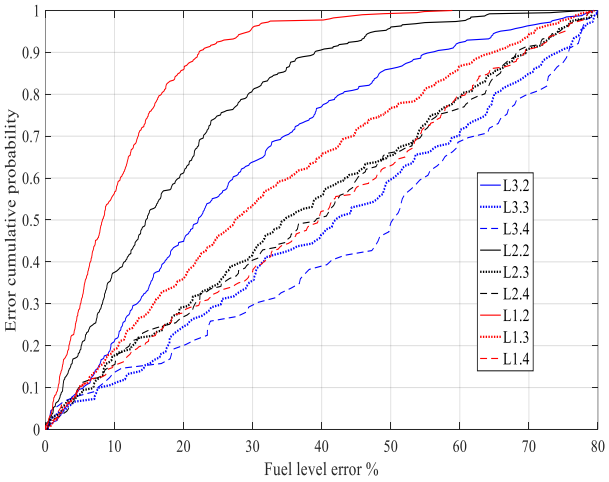

Fig. 3 Error cumulative probability for light sensors

Copyright ©2018 by the International Astronautical Federation (IAF). All rights reserved.

References

[1] Zhumaev, Z.S., Vlaskin, A.L., Sivkov, A.S. and Zharkikh, R.N., Sputnix education: From satellite mockup to cubesat launch, Advances in the Astronautical Sciences (2018) 461-465.

[2] Hakima, H., Bazzocchi, M.C.F. and Emami, M.R., A deorbiter CubeSat for active orbital debris removal, Advances in Space Research, 61(9) (2018) 2377-2392.

[3] Dono, A., Plice, L., Mueting, J., Conn, T. and HO, M., Propulsion trade studies for spacecraft swarm mission design, IEEE Aerospace Conference Proceedings 2018, pp. 1-12.

[4] Gomez Jenkins, M., Krejci, D. and Lozano, P., 2018. CubeSat constellation management using Ionic Liquid Electrospray Propulsion. Acta Astronautica, 151, pp. 243-252.

[5] Ranjan, R., Karthikeyan, K., Riaz, F. and Chou, S.K., Cold gas propulsion microthruster for feed gas utilization in micro satellites. Applied Energy, 220, pp. 921-933.

[6] Phylonin, O. and Belokonov, I., The Small-size Ionic-plasma Engine for Nanosatellites, Procedia Engineering 2017, pp. 373-379.

[7] Martin Langer, Jasper Bouwmeester Reliability of CubeSats – Statistical Data, Developers' Beliefs and the Way Forward https://digitalcommons.usu.edu/cgi/viewcontent.cgi?article=3397&context=smallsat

[8] Suo, M., Chen, X. and Li, S., Identification of mass characteristic parameters for spacecraft based on differential evolution algorithm, Proceedings - 5th International Conference on Instrumentation and Measurement, Computer, Communication, and Control, IMCCC 2015 2016, pp. 1967-1971.

[9] Banit, Y.R., Belyaev, M.Y., Dobrinskaya, T.A., Efimov, N.I., Sazonov, V.V. and Stazhkov, V.M., 2005. Determination of the inertia tensor of the International Space Station on the basis of telemetry data. Cosmic Research, 43(2), pp. 131-142.

[10] Abrashkin, V.I., Voronov, K.E., Piyakov, A.V., Puzin, Y.Y., Sazonov, V.V., Semkin, N.D., Filippov, A.S. and Chebukov, S.Y., 2015. Uncontrolled attitude motion of the small satellite Aist. Cosmic Research, 53(5), pp. 360-373.

[11] Abrashkin, V.I., Voronov, K.E., Piyakov, A.V., Puzin, Y.Y., Sazonov, V.V., Semkin, N.D., Filippov, A.S. and Chebukov, S.Y., 2017. Uncontrolled rotational motion of the Aist small spacecraft prototype. Cosmic Research, 55(2), pp. 128-141.

[12] Belokonov, I. and Ivliev, A., Development of a Propulsion System for a Maneuvering Module of a Low-orbit Nanosatellite, Procedia Engineering 2017, pp. 366-372.

[13] Kozlov L.V., Nusinov M.D., Akishin A.I. Modelirovanie teplovykh rezhimov kosmicheskogo apparata i okruzhayushhej ego sredy. Moskva: Mashinostroenie, 1971.

[14] Storn R., Price K. Differential Evolution - A simple and efficient adaptive scheme for global optimization over continuous spaces, International Computer Science Institute, Berkeley, 1995